Innovative Infrastructure Solutions (2020) 5:30
https://doi.org/10.1007/s41062-020-0281-5

TECHNICAL PAPER

Treatment of an expansive soil using vegetable (DISS) fibre

Abderrahim Gheris[1] · **Adam Hamrouni**[1]

Received: 13 November 2019 / Accepted: 23 February 2020

Abstract
This paper presents the study of treatment of an expansive soil with vegetal fibres. The soil studied is swelling clay from the region of Souk Ahras (Algeria). The use of fibres as reinforcement has shown a certain efficiency which increases the bond between the soil grains due to the friction between the soil particles and the fibre material. The vegetal fibres used are DISS crushed fibres. The influence of the vegetable fibre content on the global behaviour of the soil is studied; by highlighting the role of the inclusion rate of fibre in the soil mass (1, 2 and 3% of content by weight), this will be studied by a series of behaviour and mechanical performance tests. The DISS fibres have undergone chemical-thermal treatment to extract the sugars and soluble substances contained in the vegetal to avoid the decomposition of the latter in the soil. The results will be compared to those of unreinforced soil. Experimental results show that the swelling potentials are reduced by the addition of vegetal fibres, the cohesion of the soil treated is increased, and the soil is more ductile. It has also been shown that 2% of the DISS fibre content is a critical value for reducing the swelling potential of the clay soil.

Keywords Swelling · Clay · Experimental characterizations · Soil improvement · Vegetal fibre · DISS fibre

Introduction

In the literature, there is a wide use of stabilization of swelling soils to improve their mechanical and physical properties (swelling, permeability and strength) by the addition of cement [1–3], fly ash [4–8], cement kiln dust and lime [9, 10]. Lime-treated soils have been used as materials in pavement and sub-base construction. The stabilization of expansive soils by lime has been widely used to improve the mechanical and physical properties of the soil [11]. For the improvement of the mechanical properties of expansive soils, the use of lime with sea water as a stabilizer has given good results. Furthermore, several studies have shown the high impact of sea water on the mechanical behaviour of expansive soils [12–15].

The stabilization of soils with the help of plant fibres in order to improve their mechanical characteristics has been recognized for more than 5000 years. The first two existing examples of plant fibre reinforced soil are at the ziggurats of Babylon in the ancient city of Dur-Kurigalzu, now known as Agar-Quf (Iraq), and at the Great Wall of China [16]. The Babylonians used woven reed mats and braided ropes as reinforcements. In the Great Wall of China, tree branches were used to reinforce the earth.

The incorporation of plant fibres as reinforcements in a matrix presents a large number of advantages that make it possible to combine environmental and technical performance. To this end, several studies and systematic research have focused on the role of plant fibres such as coconut [17], jute [18], palm [19, 20], sisal [21, 22] and esparto [23] on the improvement of soil mechanical characteristics. Their use, either as a component of eco-geotextiles or mixed with soils to form a composite material, has recently met with some success in the field of construction engineering (soil and embankment stability, erosion control, infiltration, etc.) as a substitute for the synthetic reinforcing fibres used in geotextiles in particular [24–26].

The influence of plant fibres on the properties of compacted soils used for road construction has been studied by several authors. Santhi et al. [22] carried out compaction tests at optimum normal Proctor (ONP) conditions on very plastic clay mixed with sisal fibres by varying their length (1.5–3 cm) and percentage (0.25–1%). The authors found that the optimal moisture content (OMC) increased relative to untreated soil and the maximum dry density decreased

✉ Adam Hamrouni
hamrouni.adam@yahoo.fr

[1] Laboratory InfraRES, Mohammed Cherif Messaadia University, Souk Ahras, Algeria

Published online: 03 March 2020

with increasing length and fibre content. Ghavami et al. [21] found that the inclusion of 4% sisal or coconut fibre conferred significant ductility and slightly increased the compressive strength of raw earth for the manufacture of building blocks. Sivakumar Babu et al. [27] investigated the effect of coir fibres on improving the shear strength parameters of silty sand on triaxial paths. They found that the optimum fibre content corresponding to a maximum strength improvement was 2–2.5% for a length of 15–25 mm. They also observed that the stiffness was generally greater than the stiffness of the raw soil at each level of deformation. More recently, Khelifi [23] studied the behaviour of silt soils reinforced by the vegetal incorporation of esparto grass, an abundant plant in Algeria. It was found that a 2% percentage of sheets embedded in the silt matrix increased the value of the deviator stress by 8% in the case of cut sheets and by 15% in the case of crushed leaves compared to silt alone.

This paper presents a study of the treatment of an expansive soil by the incorporation of plant fibres of another plant very common in Algeria called DISS. The soil under study was swelling clay from the Souk Ahras region of eastern Algeria. The use of these fibres as a reinforcement has shown some effectiveness in increasing the bond between the grains due to the friction between the soil particles and the surface of the fibres. The plant fibres used were crushed DISS fibres. The influence of the plant fibre content on the mechanical behaviour in general (direct shear strength, compaction and uniaxial compressive strength) and on the swelling in particular is studied by highlighting the effect of the variation in the percentage of fibres (1, 2 and 3% content by weight) incorporated in the clay mass. Before use, the crushed fibres underwent a chemical-thermal treatment to extract sugars and soluble substances contained in the plant in order to avoid the decomposition of the latter in the soil.

Methodology

Description of the site

The wilaya (province) of Souk Ahras is located about 700 kilometres southeast of the capital Algiers. It is characterized by high altitude and rugged terrain. The area studied is located to the south of the capital of the wilaya of Souk Ahras, and it is an old kaolinite clay deposit used in the manufacture of fired red brick, which covers an area of 14 hectares. The geographical position of the sampling site according to UTM (Universal Transverse Mercator) coordinates is $X = 406{,}625.02$ E and $Y = 4{,}009{,}119.29$ N. The average altitude of the site is $Z = 781$ m. Figure 1 shows the location of the test area [28].

Materials and methods

The clay samples were collected by core sampling in the study area south of the Souk Ahras locality (Fig. 1). In the first step, they were analysed for identification according to the usual geotechnical testing (Fig. 2). Particle size analysis was performed by wet sieving according to [29]. For particles less than 80 µm in diameter, the sedimentometric technique [30] was used. The plasticity of the soil was identified by the Atterberg limits according to the standard [31]. We used constant charge permeametry to determine the permeability coefficient of the clay. The mechanical properties of the clay, which were internal friction angle and cohesion, were determined using a rectilinear shear box [32]. Volume changes due to swelling were identified by an automatic computer-controlled oedometer equipped with a high-precision strain sensor and a 5 kN capacity load cell [33].

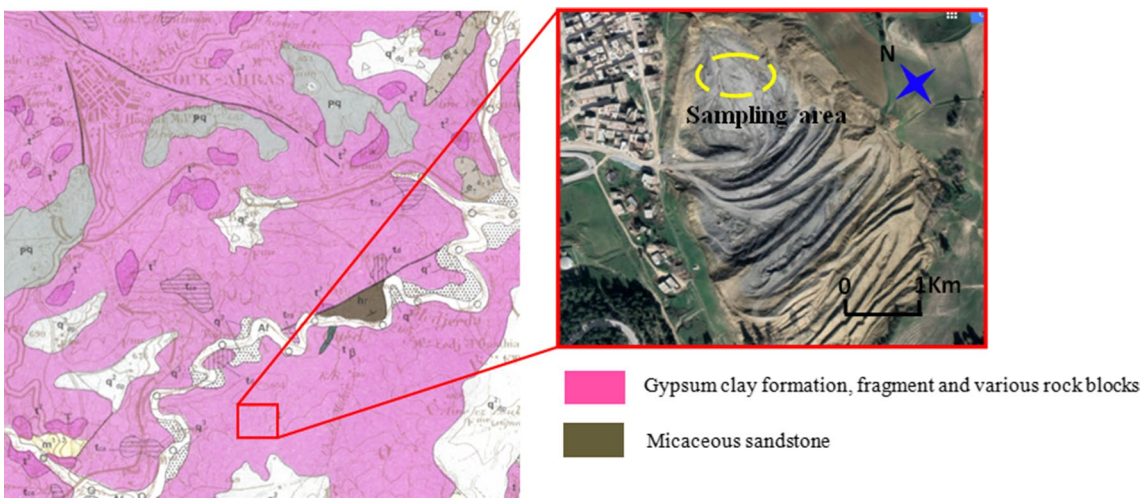

Fig. 1 Geological map of Souk Ahras region, map n°77, scale 1/50,000

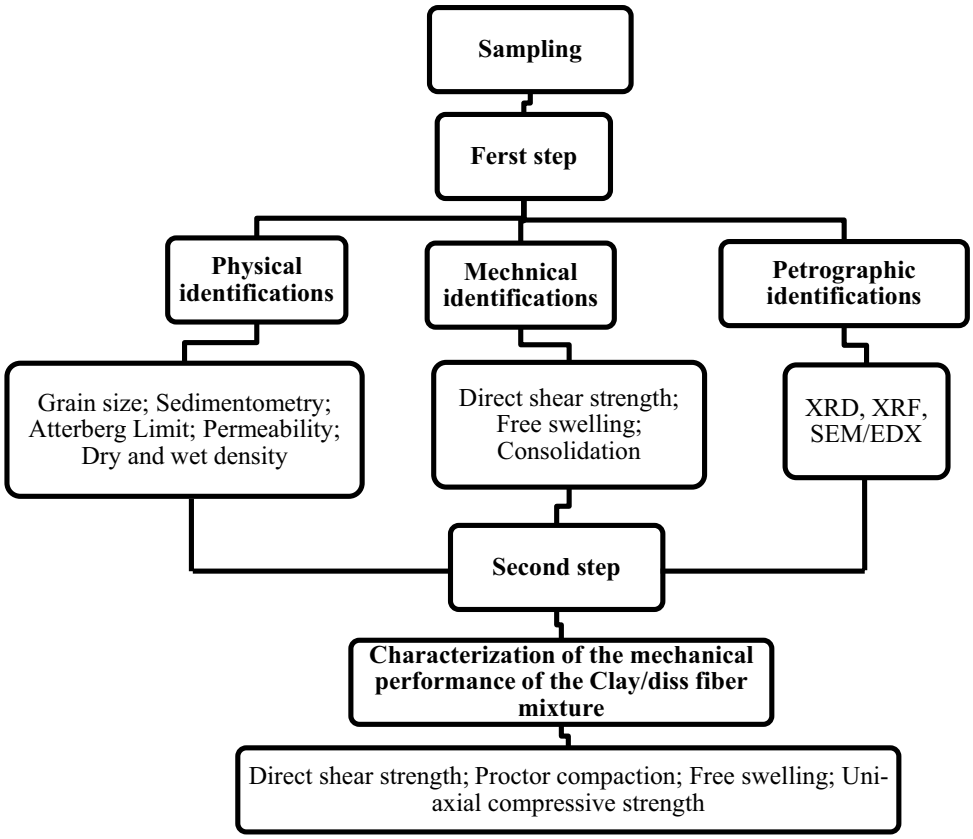

Fig. 2 Flow chart of testing programme

The mineralogical composition was obtained by X-ray diffraction (XRD) on the <2 µm fraction. The diffractometer used Cu Kα radiation (λ Cu = 0.154056 nm), a nominal tube voltage of 40 kV and a nominal current of 30 mA, and data were collected for 2θ values of 7°–90°. The *X'Pert High-Score Plus* V3.0 software program (*PANalytical*©) was used to identify the mineral phases in each X-ray powder spectrum by comparing experimental peaks with PDF2 reference patterns. Microscope imagery was performed using a stereomicroscope, while the morphology of the dried clay surface was observed with a scanning electron microscope (SEM) equipped with an SE1 probe for surface microanalyses.

The X-ray fluorescence (XRF) analysis of the clay sample was conducted using a wavelength-dispersive XRF spectrometer with an X-ray tube power of 1 kW. The analysis was performed at the Applied Research Unit in Iron and Steel Metallurgy of the Industrial Technologies Research Center (ARUSM-ITRC).

In the second part of the experiment, mechanical performance tests were carried out on the clay/DISS fibre mixtures at the adopted fibre dosages. Since these tests included the study of free swelling, we used the same apparatus as for the mechanical evaluation in the first stage (the automatic oedometer). The compaction study was performed using the Proctor normal method, which consists of compacting the clay or clay/DISS mixture in a standard mould using a standard tamper and measuring its natural water content and density after compaction, in accordance with standard [34]. Finally, for the measurement of the unconfined compressive strength, we used a semi-automatic crushing press. For data acquisition, linear variable differential transformer (LVDT) sensors for force, displacement pressure and strain were installed.

Experimental studies

The experimental study consists of experimentally characterizing the behaviour of soils reinforced with fibres from the DISS plant in order to understand their effect on the improvement of the mechanical performance of expansive soils. For this purpose, a series of tests were carried out in the laboratory. The first concerns the study of the swelling potential of the clay/DISS mixture in relation to untreated soil. The second series focuses on the characterization of the mechanical resistance (shear and uniaxial compression), as well as the performance in terms of compaction brought about by the inclusion of DISS fibres in the soil mass studied.

The vegetable fibre referred to as 'DISS'

DISS is a fibrous wild plant species (Ampelodesmos mauritanicus, family Poaceae, Fig. 3) that can be found in abundance on the Mediterranean shores [35]. This plant has long been used in handcraft applications and in the construction of earth-based eco-building [36]. This DISS fibre has a tensile strength of about 100 MPa, a density of 850 kg/m^3 and a modulus of elasticity of 2.17 GPa. The fibres contain 30% cellulose and 11% hemicellulose [35].

The outer surface of DISS raw fibre is thorny (Fig. 4), which improves adhesion when mixed with the soil. Adhesion is highly sought after as a reinforcing property. The thorns on DISS reinforcement fibres (Fig. 4) offer the advantage of naturally improving adhesion at the fibre/soil interface. The surface of the thorns is not homogeneous and is covered with a substance with a texture similar to natural wax. The surface between the thorns has visible streaks covered with fine entangled needles. In addition, electron microscopic examination reveals that the inner surface of the DISS fibre is covered with thorns of 20 µm in diameter. These thorns are evenly spaced (10 µm) and evenly distributed over the entire surface of the fibre.

Fibre pretreatment

In this work, once the DISS leaves were collected, they were washed with distilled water to remove dust, contamination and adhering dirt. Only green and unbroken leaves were selected. Next, the extremities of the leaves were cut off to keep only the central part, which is characterized by a constant diameter throughout its useful length; the leaf average diameter is ~1 mm. Next, the DISS fibres were cut manually into 10 to 15 mm sections and then dried in an oven at 60 °C for 24 h to ensure constant moisture content.

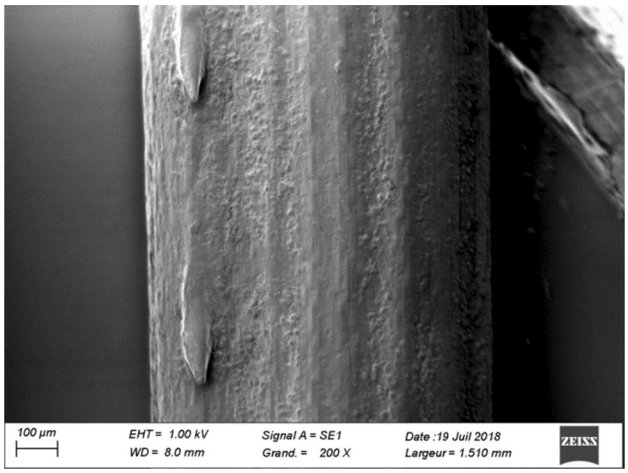

Fig. 4 The external surface of the fibre DISS, observed by SEM

Alkaline treatment with NaOH at room temperature

The fibres were soaked in a 10% NaOH solution for 30 min at room temperature, then thoroughly washed and distilled to remove traces of soda on their surface. Finally, they were dried in an oven at 60 °C for 24 h, and Boukhoulda et al. [37] have shown that alkaline treatment with a 10% NaOH concentration is the optimal treatment and gives the best resistance to the tensile test. The morphology of the fibres changes with increased NaOH concentration, the fibres become further apart, and the diameter decreases. In addition, NaOH concentration > 14% destroys the microfibrils constituting the fibre bundles leading to degraded mechanical properties. The treatment aims to prevent degradation of the plant fibre in contact with the soil.

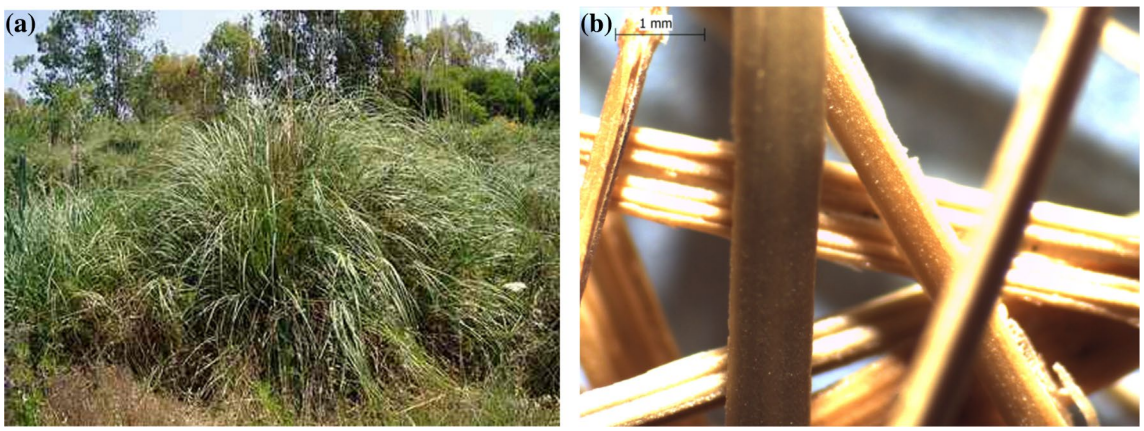

Fig. 3 The DISS fibre (Ampelodesma mauritanica); **a** the natural state, **b** the raw state

Sample preparation

Uniform fibre distribution is an important aspect of sample preparation, but a uniform fibre distribution in the soil cannot be accurately determined. The clay samples sieved through a 2-mm sieve were mixed with the DISS fibres previously cut into 10–15 mm sections in the following proportions: 1%, 2% and 3% of the weight of the dry soil. This mixture was then subjected to a series of free-swelling tests carried out according to the protocol described above in paragraph (Swelling Potential Characterizations, Direct Method), Fig. 5.

Results and discussion

Characterization of the study soil

Unaltered samples taken from the blackish clay layer at the site were subjected to physical and mechanical identification tests. The results are summarized in Table 1. The properties that were measured are as follows:

- Atterberg limits (liquidity limit, WL, and plasticity index, Ip);
- Granulometry, characterized by the percentage of grains with size < 2 µm (F2: proportion of clay % < 2 µm);
- Activity (Ac = Ip/F2);
- Natural water content (w);
- Dry bulk density (γ_d).

Fig. 5 Overall view of the sample at the end of the free-swelling test (2% mixture)

Table 1 Characteristics of the soil studied

Designation	Blackish to yellowish clay, plastic
Dry density (g/cm^3)	1.45
Wet density (g/cm^3)	1.90
Natural water content (%)	31.70
Liquidity limit (%)	52.18
Plasticity index (%)	47.97
% passing through 0.2-mm sieve	94.04
% passing through 80-µm sieve	78.42
Proportion of clay %<2 µm (F2)	65.2
Coefficient of permeability (m/s)	9.92×10^{-6}
Cohesion C_{uu} (kPa)	103.85
Internal friction angle φ_{uu} (°)	0
Cohesion C_{CD} (kPa)	68.62
Internal friction angle φ_{CD} (°)	10.75
Preconsolidation constraint (kPa)	52.50
Consolidation index C_c	0.22
Swelling index C_g	0.0504

The characteristics obtained from the tests reveal a very plastic clay soil (Atterberg limit) and a high clay activity (Ac > 0.73). The soil was not very dense or moist (Table 1).

Characterization of the swelling potential

Many methods are used for estimating the swelling potential of soil, and these can be classified into two categories.

The *indirect method* is based on correlations between several physical characterization parameters, such as Atterberg limits, with granulometry. For the clay presented in this study, the swelling potential was classified using the methods presented by the Building Research Establishment [38–41]. The results of these classifications are shown in Table 2.

Table 2 Classification of the studied soil according to its swelling potential, based on several criteria

Method of estimating the swelling potential	Classification parameters	Swelling potential
Seed et al. [40]	A_c & % < 2 µm	High
Chen et al. [39]	W_L (%) & % < 74 µm	High
BRE method [38]	I_p & % < 2 µm	Very high
Williams et al. [41]	I_p & % < 2 µm	High

A_c: activity index of clay, $A_c = I_p$/%<2 µm; I_p: plasticity index; %<2 µm: particles smaller than the 2 µm diameter; W_L: liquidity limit; %<74 µm: particles smaller than the 74 µm diameter

The *direct method* uses three parameters to describe the swelling: the rate of swelling or free swelling, defined by $A_g = dh/h_0$; the swelling pressure, σ_g, which is the pressure that must be applied to the soil sample to prevent swelling during hydration; and the swelling index, C_g, which reflects the significance of the swelling induced by unloading in relation to a given load.

Cylindrical samples were cut from the clay cores extracted from the study site, and their faces were erected to obtain flat surfaces parallel to each other and perpendicular to the sample. After being cut, the samples were subjected to the oedometer free-swelling test in accordance with standard [42]. This standard specifies that the test load should be applied for 2 h or until the variation in height of the specimen between two readings with a 1-h time interval is lower than 10 µm. Water is then introduced into the oedometric cell. A constant force is then maintained until the height levels off. Conventionally, this levelling off is considered to be reached when the variation in height is less than 1/100 mm between two readings taken 8 h apart. The experimental results are then plotted on a variation curve of the deformation dh/h_0 as a function of time.

We adopted three loads to apply to the specimens [42]. For the first specimen, we applied a load such that the average stress caused by the load and the loading device was 50 kPa. A stress equal to the earth pressure at rest, σ_{v0}, at the sampling location, which in this case was 150 kPa, was applied to the second test piece. The final load was chosen such that the points were best distributed over the range 50–150 kPa in a graphical representation, resulting in a load of 100 kPa.

Table 3 summarizes the different results of the oedometer swelling tests. As can be seen from this table, the swelling pressure was high according to the classifications of Chen and Ma [39]. According to Seed et al. [40], the swelling rate was also high ($A_g > 5\%$) at this site. Additionally, the C_g values indicate a medium-to-high swelling potential. All of these results are in agreement with those obtained from indirect classification methods.

To obtain more information on the behaviour of the clay studied after saturation, free-swelling tests were carried out according to the standard [42]. The resulting curve shows that the swelling occurs in three phases (Fig. 6):

- Initialization phase: any soil with a water content below a certain threshold will, when brought into contact with free water, draw a certain amount of this water into its pores. This phenomenon is known as sucking, and the corresponding forces are the sucking forces. This sucking behaviour subsequently causes a flow in the interstices. Once these forces are damped, inter-particle swelling begins to occur and the sample enters the primary swelling phase.
- Primary swelling phase: in this phase, inter-foliar swelling occurs massively and progressively. The clay sheets attract the water particles, resulting in significant volume deformation of the sample. The primary swelling time

Table 3 The results of swelling tests on the studied clay

	swelling stress σ_g (kPa)	Swelling rate A_g (%)	Swelling index C_g (%)
Sample	100	17.5	5.04

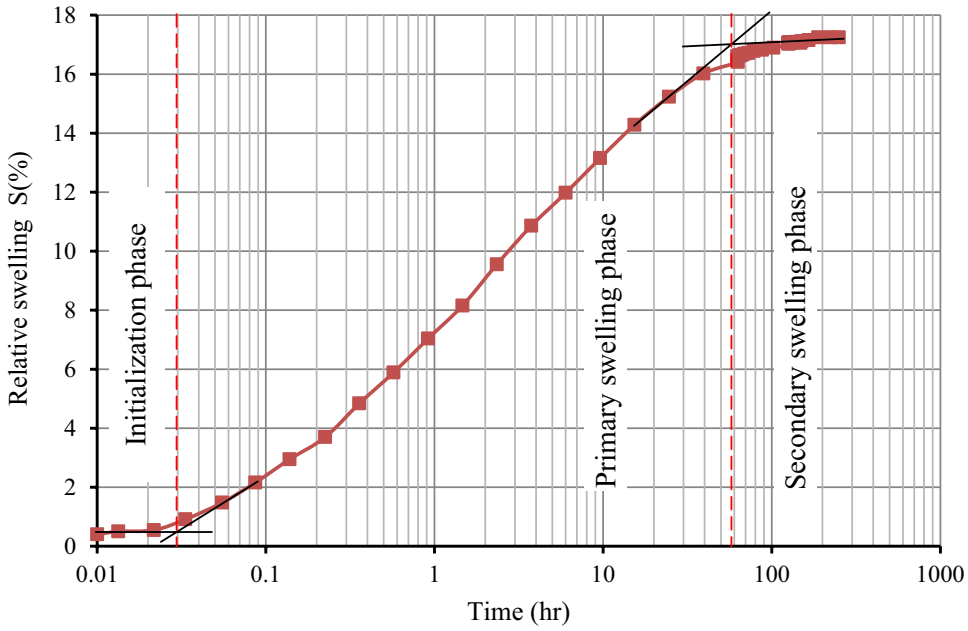

Fig. 6 Example of swelling curve made on the studied clay

depends on the granulometry, the nature of the clay minerals and the height of the sample.

- Secondary swelling phase: during this phase, a reduction in swelling is observed. The sample is completely saturated, and small further volume changes are related to particle rearrangements and the stabilization of chemical bonds. This phase can last several days.

Petrographic identification of clay minerals

To prepare the samples for chemical and mineralogical analyses (XRF and XRD), the samples collected were first crushed into pieces using a mortar and then dried in an oven for 24 h at 105 °C. Next, the pieces were ground and the resulting powder was sieved through a 50-µm mesh diameter sieve.

X-ray fluorescence

The elemental analysis of the material used was carried out at the ARUSM Laboratory of the ITRC Annaba unit. Table 4 shows the results of this analysis, which reveal the predominance of silica, calcium and aluminium.

The percentages of silica (SiO_2) and aluminium were very significant, indicating the presence of kaolinite ($Al_2Si_2O_5(OH)_4$). Furthermore, the calcium content was relatively high, showing that this material is rich in calcite ($CaCO_3$). The alumina/silica ratio (Al_2O_3/SiO_2) is an indicator of the material's permeability to moisture: the higher the ratio, the greater the permeability. In our case, this ratio is small and was found to be 0.31. This low value is in agreement with the low moisture percentage (1.41%) estimated by loss on ignition (LOI) (see Table 4). The molar ratio of SiO_2/$Al2O_3$ was 3.2 (maximal substitution of Si^{4+} by Al^{3+}), which is higher than the conventional bentonite value of 2.7. This difference indicates the presence of free quartz in the clay fraction in a large proportion [43]. The overall composition of other oxides (Fe_2O_3, MgO and K_2O) reached a percentage of 11.45%, which shows that our clay was not pure [44]. The LOI was relatively high, at around 13.23%. This may be related to the presence of carbonate and silicate minerals.

X-ray diffraction

The diffractogram was obtained from an altered sample placed directly as a powder in a conventional sample holder [45]. The XRD spectrum of the raw clay is illustrated in Fig. 7. Spectral analysis indicates that the sample was composed of 66% quartz (SiO_2), 11% calcite, 14% kaolinite, 4% sepiolite ($Mg_8(OH)_4Si_{12}O_{30}(H_2O)_{12}$) and 5% dickite ($Al_2(Si2O_5)(OH)_4(HCONH_2)$, which is a subgroup of kaolinite. The results reveal the presence of two intense peaks: one corresponding to a quartz, kaolinite and dickite mixture and the other to quartz. This implies that our clay is heterogeneous. These results are in perfect agreement with the SEM observations presented in the next section. The clay fraction of our material was composed of quartz, calcite and sepiolite as a major impurity; this confirms the results of the X-ray fluorescence analysis, which showed high proportions of quartz and calcite.

Table 4 The chemical composition elemental of the clay sample studied

Elément	SiO_2	CaO	Al_2O_3	MgO	Fe_2O_3	K_2O	P_2O_5	TiO_2	MnO_2	L.O.I
% Massique	51.22	7.219	16.012	3.220	6.25	1.986	0.044	0.740	0.070	13.23

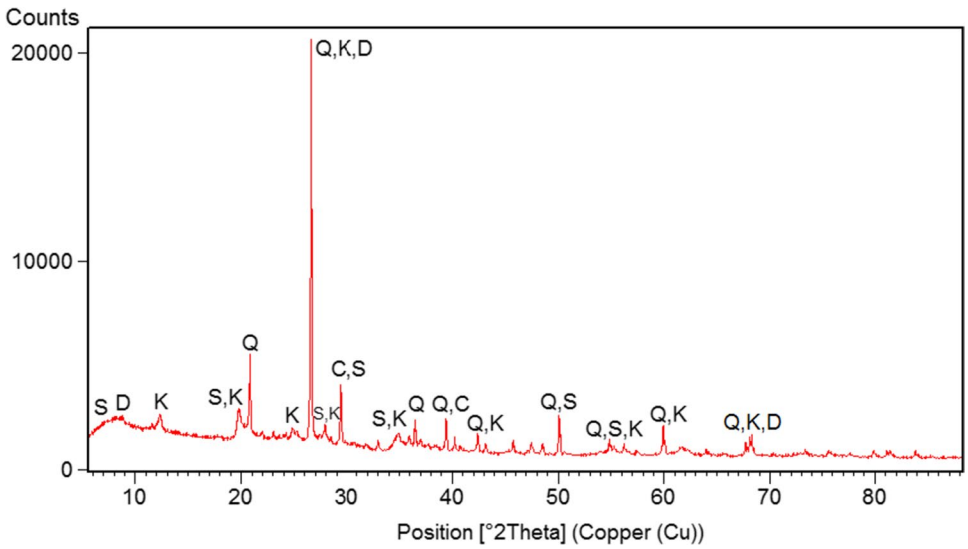

Fig. 7 X-ray diffractogram of the studied raw clay, K: kaolinite; D: dickite; Q: quartz; C: calcite; S: sepiolite

Scanning electron microscope (SEM)

Scanning microscopy allows the observation of the texture of the sample and the characterization of its mineralogical assemblages. SEM images of the clay sample at different magnifications are shown in Fig. 8. Clay particles are shown as clusters of fine aggregates and platelets in the form of irregularly shaped rods (Fig. 8c). This morphology is found in poorly crystallized kaolinites and illites, as observed by Konan [46]. The images in Fig. 8a, b are in agreement with the results of the XRD analysis, clearly showing the presence of carbonates and quartz in the sample. Carbonates (calcite) were present in the form of clearly visible aggregates, whereas quartz was in the form of small grains [47, 48].

Study of the mechanical performance of the clay/DISS mixture

Swelling as a function of time

Figures 9, 10 and 11 show the variations in relative swelling (S) with respect to time for stabilized and unstabilized expansive clays with fibre contents of 1, 2 and 3% under external pressures equal to 50, 100 and 150 kPa. For all of the mixtures, the swelling initially had a slow increase with the logarithm of time, then increased more rapidly and finally approached an asymptotic value. This behaviour corresponds to the three usual swelling stages: (1) low initial swelling due to low unsaturated hydraulic conductivity; (2) intermediate primary swelling due to a determined wetting edge; and (3) a low secondary swelling phase as conditions are near saturation. The near-equilibrium was reached in about 2–30 h for unstabilized expansive clays. The maximum swelling values (S_{max}) of the clays without added fibre were 19.98, 17.24 and 14.52% for the respective external pressures of 50, 100 and 150 kPa.

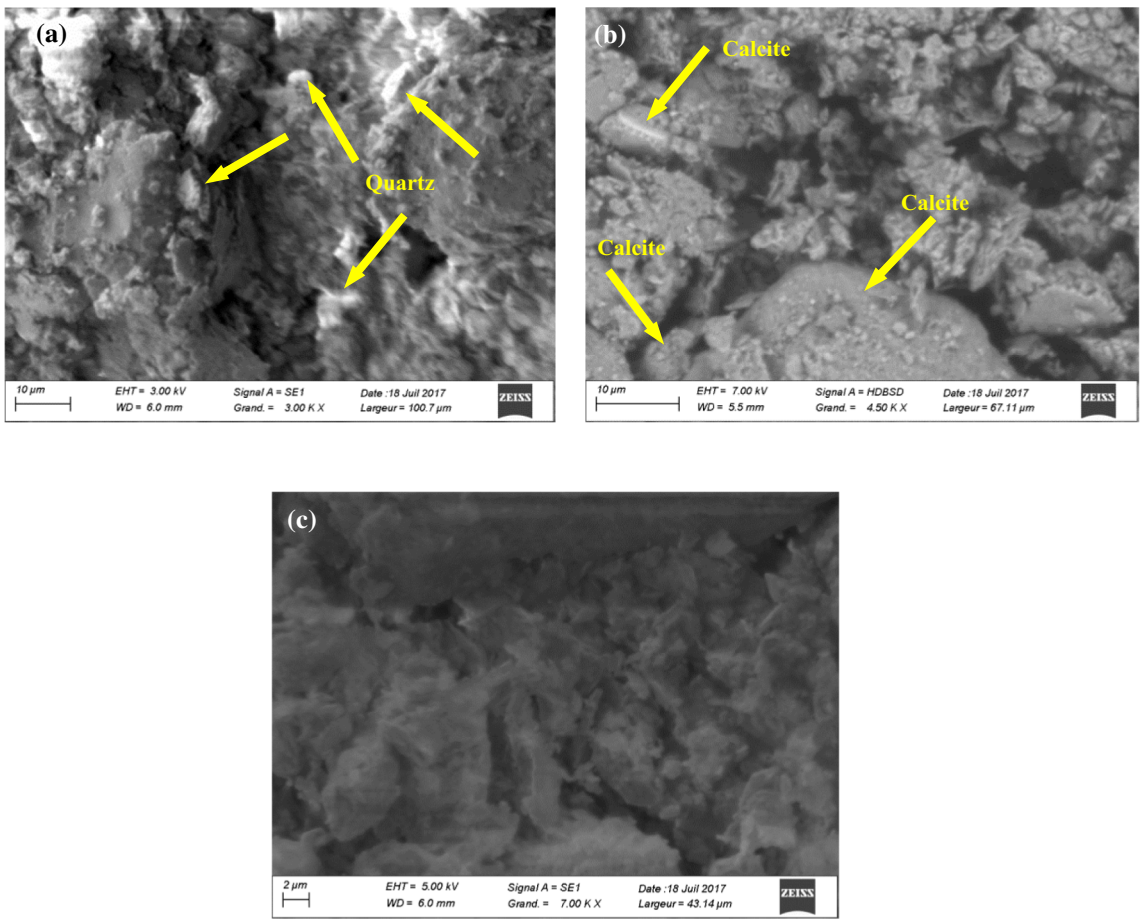

Fig. 8 **a–c** Observations with SEM of the studied raw clay

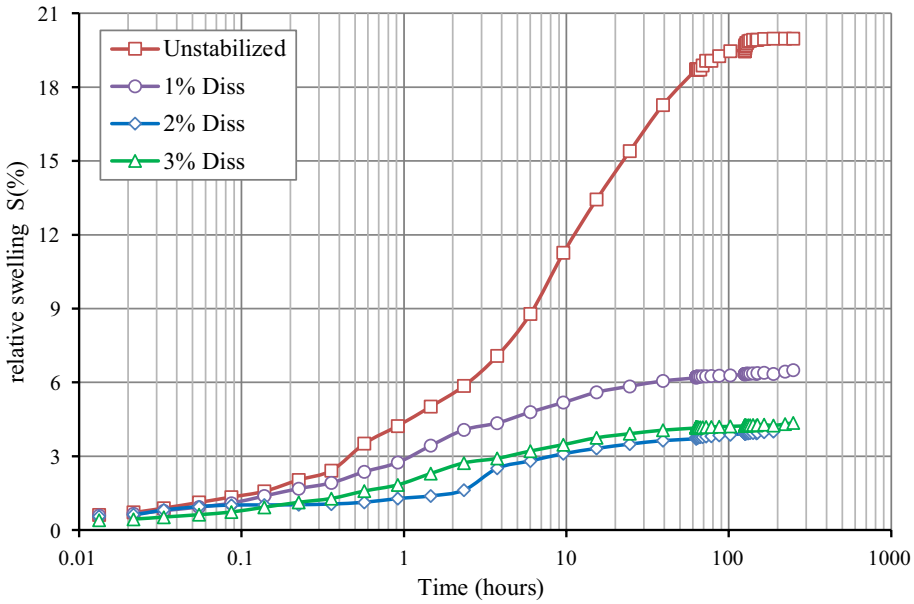

Fig. 9 Relative swelling versus time curves for unstabilized and stabilized expansive clays, under an external normal pressure of 50 kPa

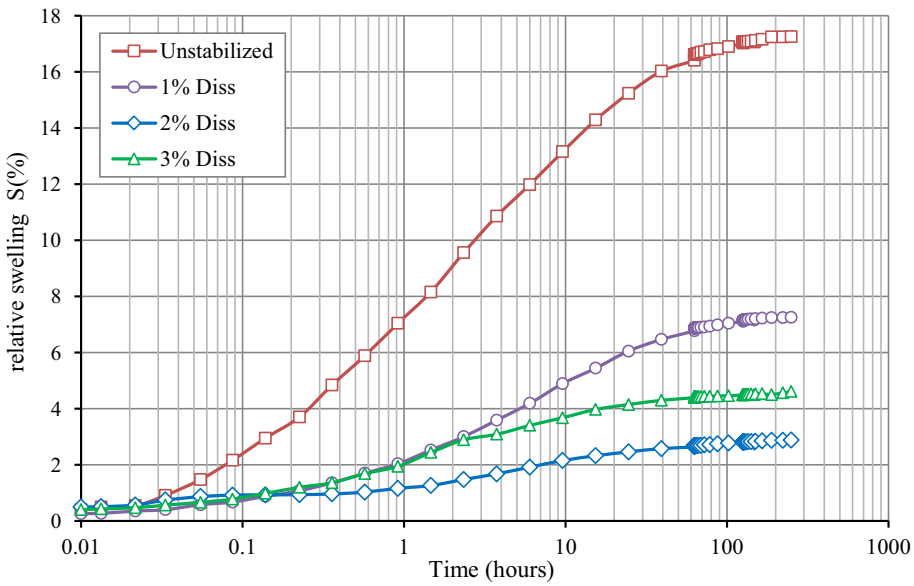

Fig. 10 Relative swelling versus time curves for unstabilized and stabilized expansive clays, under an external normal pressure of 100 kPa

The swelling volumes and times required for the stabilized clays were lower than those of the unstabilized expansive clays. The S_{max} values of the expansive clay under an external pressure of 50 kPa were 6.5, 4.25 and 4.35% for fibre contents of 1, 2 and 3%, respectively. For an external load of 100 kPa, the corresponding S_{max} values were 5.7, 3.59 and 3.9%, while for an external pressure of 150 kPa, they were 4.47, 1.81 and 2.79%. The time required to reach near-equilibrium was only about 100–200 h.

Characterization of the behaviour clay/fibre mixture during swelling

Sazhin [49] developed a model of a swelling soil by considering springs precompressed by an applied load. For low values of the applied load, the author recommends determining the value of the swelling pressure using the following formula:

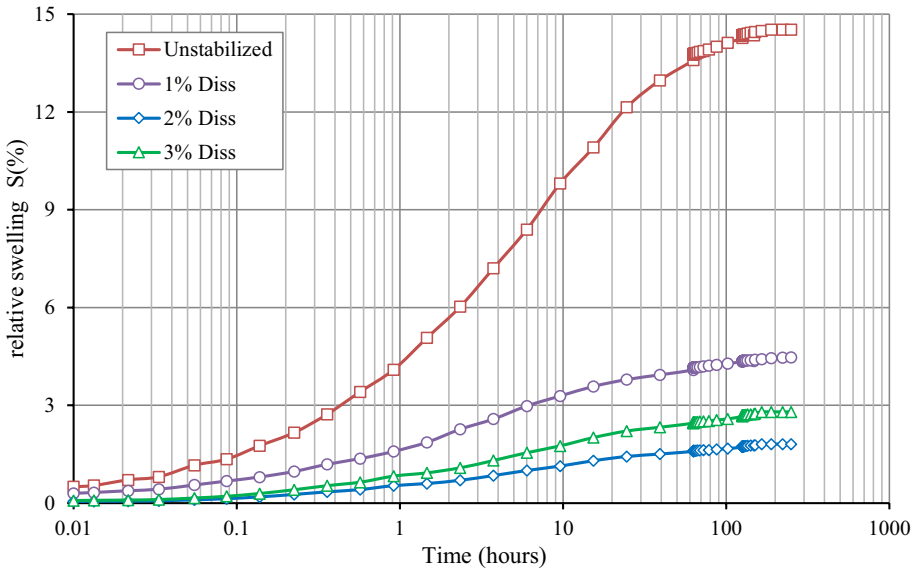

Fig. 11 Relative swelling versus time curves for unstabilized and stabilized expansive clays, under an external normal pressure of 150 kPa

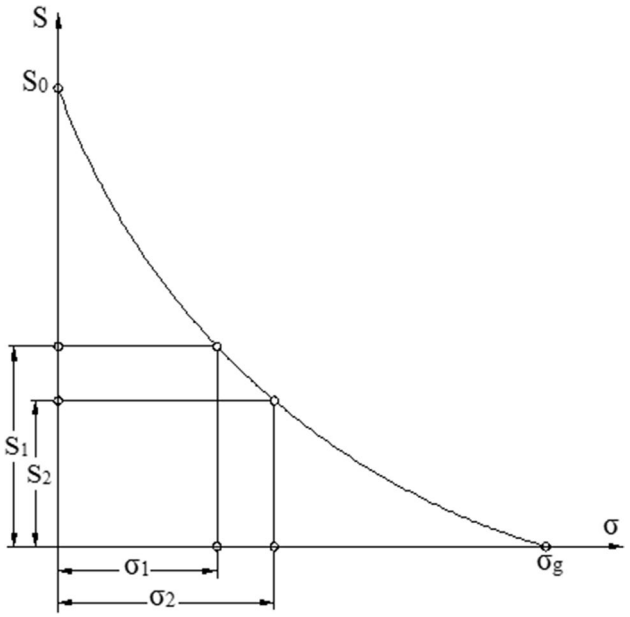

Fig. 12 Determination of the proportionality coefficient k from a swelling test, Sazhin [49]

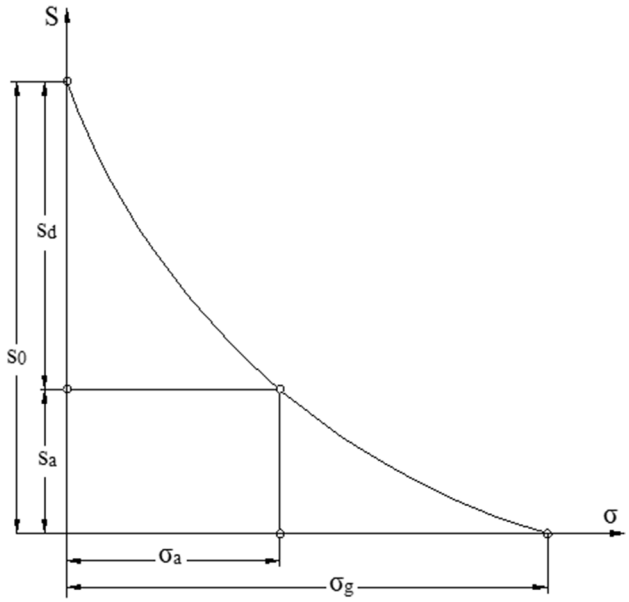

Fig. 13 General form of a swelling test [51]

$$\sigma_g = \sigma_a + s \cdot k \tag{1}$$

where σ_g is the ground swelling pressure, σ_a is the external pressure at which the foundation heave is determined, s is the vertical deformation of the ground during swelling, and k is a proportionality coefficient that depends on the foundation width and the embedding depths of the foundation and the active ground swelling zone. The value of the modulus, k, is deduced from Eq. (2)

$$k = \frac{\sigma_2 - \sigma_1}{s_1 - s_2} \tag{2}$$

where s_1 and s_2 are the amplitudes, in absolute values, of the ground uplift under the pressures σ_1 and σ_2, respectively (Fig. 12).

The question of determining the value of the reaction modulus of swelling soils has been studied by [50, 51]. To determine the soil reaction modulus, an experimental curve obtained in the laboratory that reflects the relationship between the amplitude, s, of the soil swelling and the applied pressure, σ_a, is used. The difference between the swelling of

Table 5 Maximum swelling amplitude of the clay alone and mixed with the DISS fibre, extracted according to Figs. 9, 10 and 11

s_a (mm)	σ_a (kPa)		
	50	100	150
Clay alone	3.996	3.448	2.905
Clay + 1% DISS	1.300	1.150	0.894
Clay + 2% DISS	0.857	0.574	0.362
Clay + 3% DISS	0.871	0.722	0.559

the ground under the action of a non-zero restrictive pressure ($\sigma_a \neq 0$) and the free swelling that occurs without restrictive pressure ($\sigma_a = 0$) is designated as the 'swelling deficit' [51]. The swelling deficit is shown in Fig. 13, and its value is determined by Eq. (3).

$$s_d = s_0 - s_a \tag{3}$$

Thus, Lytton [50] proposes that to calculate the soil reaction modulus using Eq. (4), the terms σ_1, σ_2 and $(s_1 - s_2)$ in Eq. (2) are replaced with σ_a, 0 and $\left(s_d = s_0 - s_a\right)$, respectively:

$$k = \frac{\sigma_a}{s_0 - s_a} \tag{4}$$

where σ_a is the external pressure applied to the specimen, s_a is the amplitude of the swelling of the ground under the pressure σ_a, and s_0 is the amplitude of the free swelling of the ground with zero pressure.

Table 5 shows the results of the maximum swelling amplitudes, s_a (gross displacement), extracted from the results of the free-swelling test shown in Figs. 9, 10 and 11 for the clay alone and for the clay mixed with DISS fibre.

Table 6 Value of the free-swelling s_0, for a zero external pressure $\sigma_a = 0$

	s_0 (mm)
Clay alone	4.705
Clay + 1% DISS	1.602
Clay + 2% DISS	1.332
Clay + 3% DISS	1.100

Table 7 Values of the soil reaction modulus of the clay/DISS mixture, according to the external pressure

k (kPa/mm)	σ_a (kPa)		
	50	100	150
Clay only	70.522	79.554	83.333
Clay + 1% DISS	165.562	221.239	211.864
Clay + 2% DISS	105.263	131.926	154.639
Clay + 3% DISS	218.34	264.55	277.264

In order to determine the free swelling, s_0, we used the results of Table 5 in order to visualize the trend curves of the variation of the swelling, s_a, as a function of the external pressure, σ_a, for each type of clay/DISS mixture. Figure 14 shows the resulting trend lines. We find that the correlation coefficients are good ($R^2 > 0.96$). Therefore, the value of s_0 was calculated by setting the value of σ_a to zero in each trend equation. Table 6 presents the resulting values of s_0.

Finally, using Eq. (4) and the data in Tables 5 and 6, we obtain the values of the modulus, k (kPa/mm), which are summarized in Table 7.

Figure 15 shows the change in swelling pressure determined by Eq. (1) with, respect to the fibre content, the external pressure, and the value of $s = s_a$ corresponding to the external pressure (Table 5). In general, it can be observed that the effect of including the DISS fibre significantly

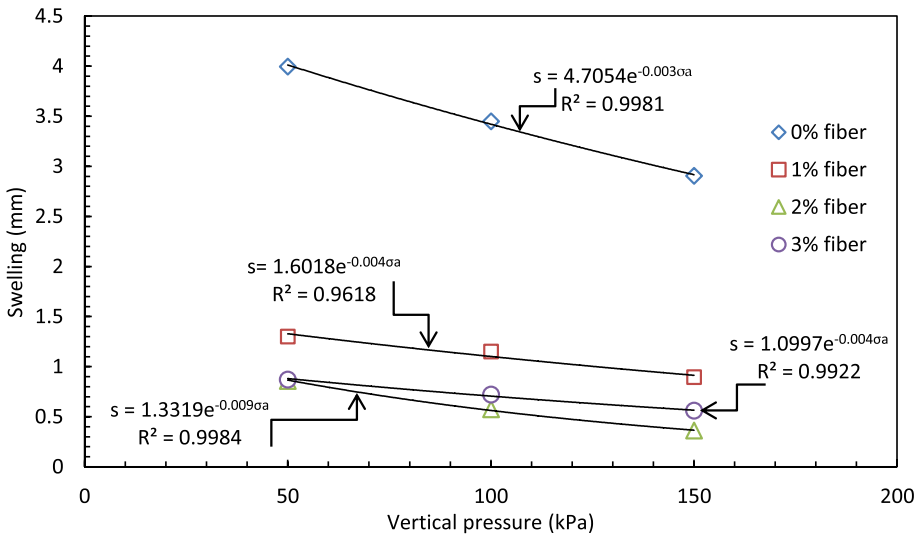

Fig. 14 Relationship between vertical external pressure and swelling

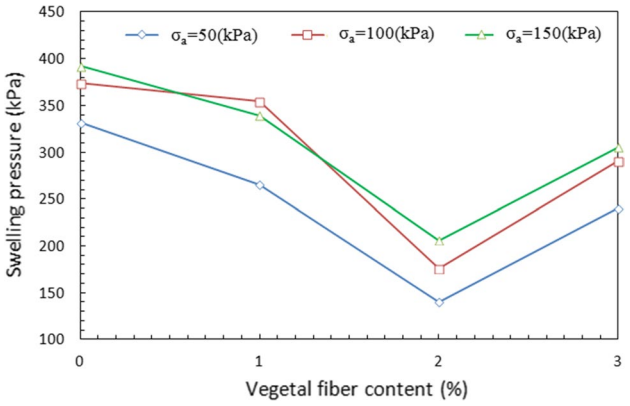

Fig. 15 Variation of the swelling pressure according to the DISS fibre dosing

reduced the swelling pressure, regardless of the rate of incorporation. In addition, we have found that 2% is the optimal value that gives the best results in terms of swelling pressure reduction.

Effects of fibre content on S_{max} The effects of the fibre content on the change in swelling (S_{max}) of stabilized expanded clays under external pressures of 50, 100 and 150 kPa are shown in Fig. 16. We can see that the S_{max} of the expansive clays under pressures of 50 and 100 kPa decreased rapidly when the fibre content increased from 0 to 1%, decreased slightly when this percentage increased to 2% and finally remained more or less constant, with a slight increase for a fibre content of 3%.

Thus, 2% is considered to be the optimal value, regardless of the value of the external pressure, σ_a. According to Fig. 16, the S_{max} values for untreated clays were 19.98, 17.24 and 14.52% for external pressures of 50, 100 and 150 kPa, respectively, while the corresponding S_{max} values for clays

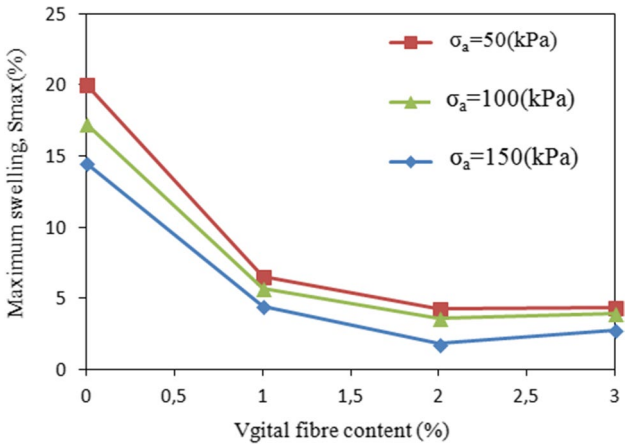

Fig. 16 The effect of the DISS fibre content on change in the S_{max} value according to the vertical external pressure σ_a

treated with the optimum fibre content of 2% were 4.25, 3.59 and 1.81%. This corresponds to a reduction in swelling of 78.73, 79.18 and 87.54% compared to the untreated soils for external pressures of 50, 100 and 150 kPa, respectively. This finding is consistent with the work of Dasaka et al. [17], who studied the influence of the addition of coconut fibres on the compressibility and swelling index of a clay soil. They found that swelling was reduced by about 40% when the fibre content was 0.5–1.5%. A maximum reduction was found when the fibre content was between 1 and 1.5%.

Influence of plant fibres on compaction properties

In this section, we investigate the effects of the incorporation of DISS plant fibres on the change in compaction parameters of a clay soil. Among other things, the parameters of the optimum Proctor conditions, including the optimum dry density and optimum water content, were studied. For this purpose, we carried out compaction tests at the optimum normal Proctor (OPN) conditions on the clay alone and then mixed with the DISS fibre at different dosages (1.2 and 3%). The tests were carried out according to the standard [34].

As shown in Fig. 17, we see that an increase in fibre content caused a decrease in the maximum dry density of about 6.21% and, on the other hand, increased the optimal moisture content by 21.43% compared to untreated clay. This finding has been confirmed by several authors. Santhi et al. [22] carried out compaction tests at ONP on a very plastic clay mixed with sisal fibres by varying their percentages in the range of 0.25–1%. The authors found that the optimal moisture content increased relative to untreated soil (OMC increases by 60% compared to the untreated soil, Fig. 18), while the maximum dry density decreased with increasing fibre content (around 5.06%, Fig. 19). Similarly, Marandi et al. [20] found a decrease in the maximum dry density and an increase in the optimal moisture content when adding palm fibres at 0.5 and 1% to a silty sand matrix. The

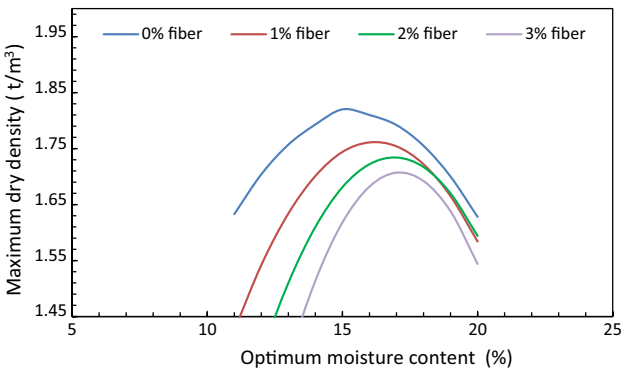

Fig. 17 Result of the normal Proctor, for different Clay/DISS mixtures

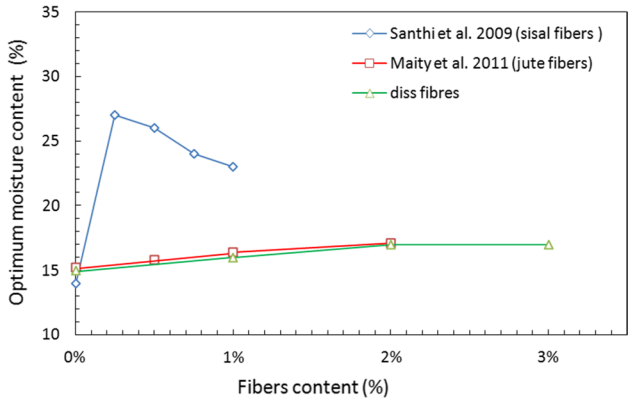

Fig. 18 Variation of the optimal moisture content in function of the fibre dosage, according to several types of fibres

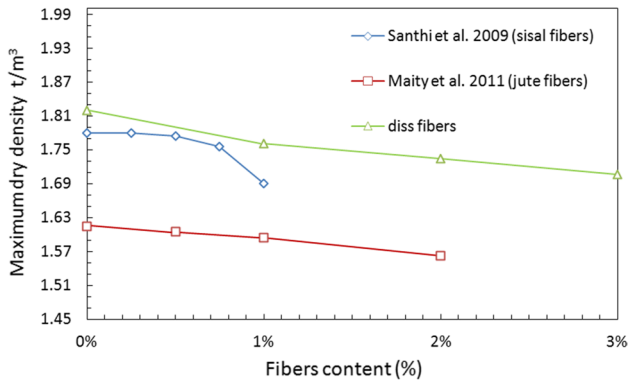

Fig. 19 Variation of the maximum dry density in function of the fibre dosage, according to several types of fibres

same result was found by Maity et al. [18] for two types of sand mixed with 0.5–2% jute and coir fibres (decrease of the maximum dry density about 3.22% and increase of the optimal moisture content of 13.33%). Figures 18 and 19 show a comparison of our results with some work available in the literature.

The decrease in dry density observed in Fig. 19 can be explained by the low specific gravity of the fibre filaments compared to the soil grains and by the tendency of the fibres to keep the soil particles away from each other. Furthermore, the increase in the optimal water content is probably due to the higher water absorption capacity (hydrophilicity) of the fibres compared to the soil.

Shear strength of the clay/fibre mixture

Direct shear tests were carried out to study the shear strength of the soil treated with added DISS plant fibres. This strength was characterized by the cohesion and the internal angle of friction. For this purpose, several clay/DISS mixtures were prepared in the usual dosages of 1.2 and 3%. Cylindrical specimens with dimensions 85 × 170 mm were made by compaction. A paper and plastic were placed inside the moulds to prevent the clay from sticking to the walls. The specimens were compacted under the conditions of the OPN of the unaltered clay, which were a maximum dry density (γ_{dmax}) of 1.82 and optimum moisture content (w_{omc}) of 15%.

First, a reference shear test was carried out on the clay without added DISS in order to characterize its mechanical behaviour. The direct shear tests were carried out according to the standard [32] on samples cut in the shear of box format from the manufactured cylindrical specimens. The internal dimensions of the shear box used in our study were a length of 60 mm, a width of 60 mm and a height of 20 mm. The tests were carried out in consolidated and drained modes (the consolidation stress was applied in such a way as to have a maximum dry density γ_{dmax}=1.82) at a speed of 0.002 mm/min under normal stresses of 100, 200 and 300 kPa.

The evolution of the shear strength of the clay with respect to the horizontal displacement under the three normal stresses applied is shown in Fig. 20.

As seen in Fig. 20, after stabilization of the shear rate, the curve $\tau = f(\Delta l)$ shows a linear slope which increases with normal stress. In addition, the shear stress presents a peak of maximum strength (τ_{max}), followed by a decrease to a horizontal plateau corresponding to the critical (or residual) shear stress. It can be seen that the shear stress reaches a maximum strength level, although this is not very obvious in the case of the normal stress of 300 kPa as shown in Fig. 20b, c.

Table 8 shows the variation in cohesion and angle of friction of the reinforced soil with respect to the fibre percentage. We note that a remarkable decrease in the angle of friction between 0 and 2% added fibre contents was followed by a relative stabilization (Fig. 21) around 2 to 3%. This decrease is partially compensated by an increase in cohesion.

It can also be noted that the cohesion had significant increases as the fibre contents increased to 2%. There was then a slight increase to reach a maximum value for dosages above 2%. This increase can be explained by the presence of a kind of claw on the surface of the DISS fibres (Fig. 4) that binds the soil particles together.

It is also important to note that the variations in cohesion and angle of friction as functions of the percentage of natural fibres incorporated into the soil matrix were non-linear. We were unable to test fibre contents higher than 3% due to the difficulty of sample preparation beyond this percentage.

Uniaxial compressive strength

For the purpose of determining the compressive strength of the clay/DISS mixture, specimens were prepared

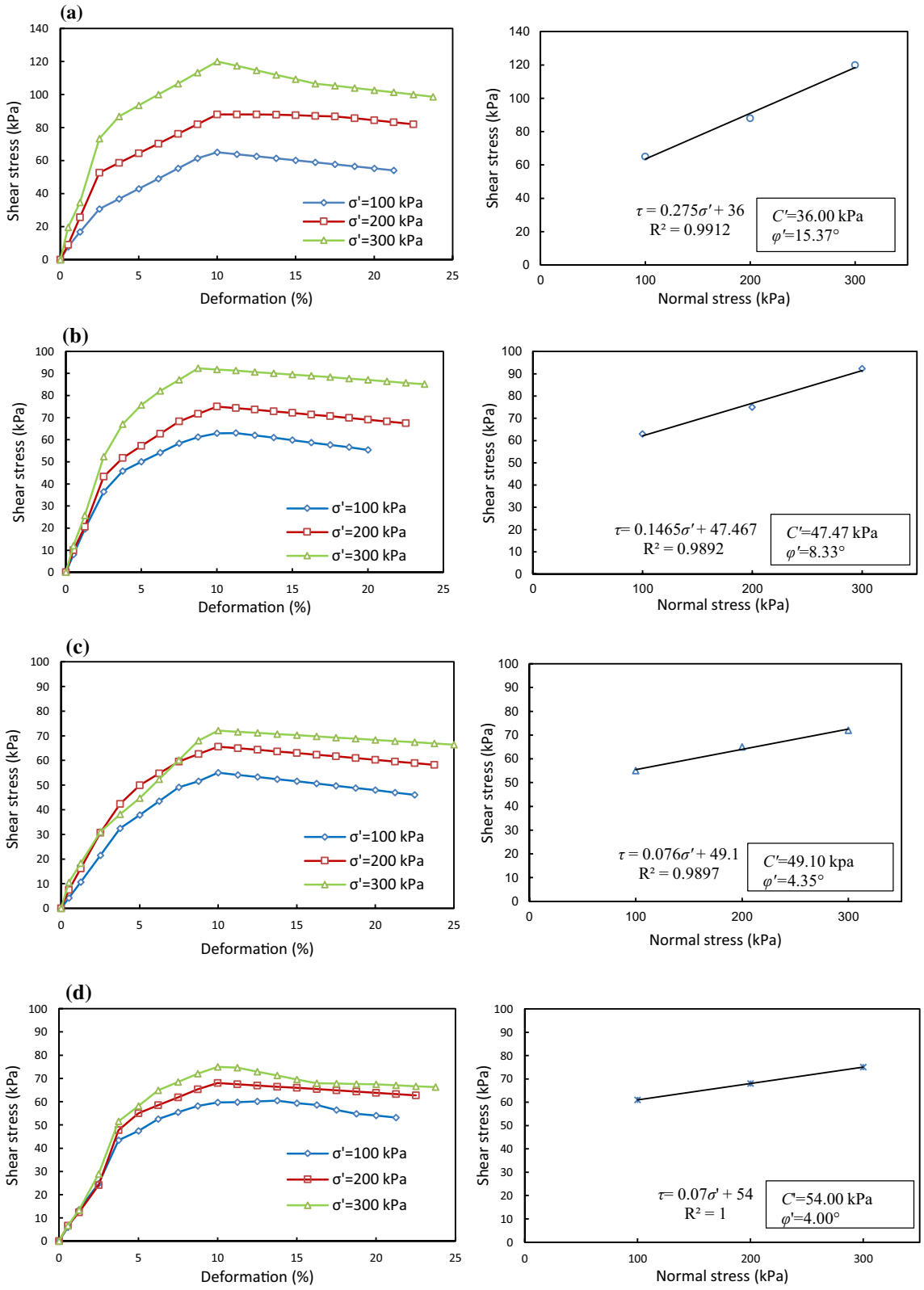

Fig. 20 Horizontal displacement curve and Mohr–Coulomb model of rupture for: **a** clay alone; **b–d** clay/DISS mixture according to dosages (1.2 and 3%), respectively

Table 8 Variation of cohesion and angle of friction as a function of the percentage of DISS fibres

	Reference sample	1% Fibre	2% Fibre	3% Fibre
Cohesion C' (kPa)	36.00	47.47	49.10	54.00
Angle of friction φ' (°)	15.37	8.33	4.35	4.00

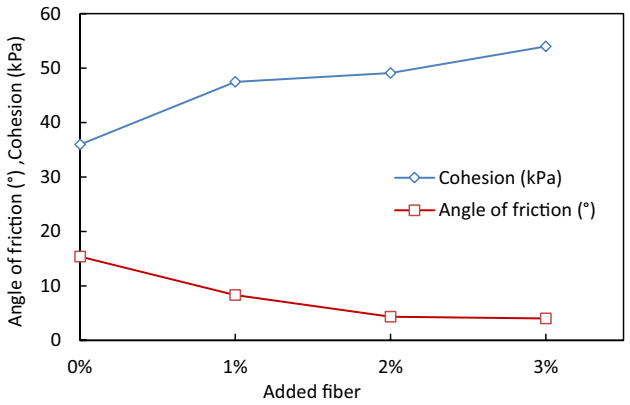

Fig. 21 Evolution of cohesion and angle of friction, with the fibres dosing

according to the same method adopted for the shear strength measurements. Each specimen was placed on the plate of a semi-automatic compression press with a loading speed of 1.6 mm/min. The press consisted of two pistons: a fixed upper piston, on which a 60 kN force sensor was placed which recorded the forces applied to the sample; and a movable lower piston. Two steel discs were placed such that one was above and one was below the specimen to distribute the pressure on the specimen. An electronic displacement LVDT sensor connected to a data acquisition unit was attached to the lower piston to evaluate the deformation of the sample during crushing. Both sensors (pressure and displacement) started recording at the moment the upper piston touched the specimen and stopped when the specimen ruptured. For each type of mixture, three specimens were prepared to allow for the calculation of the mean value of the stress and strain.

Through the results obtained, we see that the clay stabilized by the DISS fibre gave unsatisfactory values for compressive strength. For example, clay stabilized with 1% fibre had a 41.56% decrease in simple compressive strength compared to non-stabilized clay. At a fibre content of 2%, there was a decrease of 60.52%, while the 3% fibre specimens decreased by 64.93% (Fig. 22) compared to the reference. This remarkable drop in the compressive strength is probably due to the low dry density of the optimum Proctor conditions for the different clay/DISS mixtures. On the other hand, we note that the effects of incorporating the DISS fibres into the clay mass included a better ductility. Abakar et al. [52], who studied the effect of the incorporation of gum Arabic on the mechanical characterization of Ndjamena clay, obtained compressive strengths that varied between 1.67 and 3.25 MPa with an improvement of 222% for an optimal dosage of 7% gum Arabic. The authors succeeded in demonstrating a certain proportionality between the increase in dry densities of the different mixtures provided by gum Arabic and the compressive strengths.

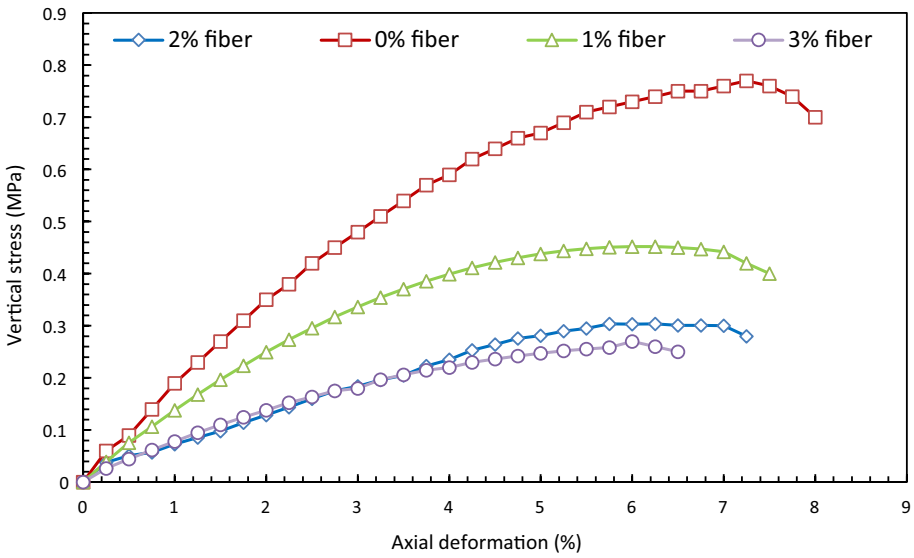

Fig. 22 Uniaxial compression test results for different clay/DISS mixtures

Conclusion

This experimental work presents an attempt to understand the behaviour of an expansive clay stabilized with DISS plant fibres. First, the clay was subjected to a physicomechanical and mineralogical identification analysis, which revealed the high degree of plasticity of the soil and showed that it consists mainly of kaolinite as an associated clay mineral. Subsequently, a mechanical performance testing series was conducted on the clay/DISS mixtures by varying the proportion of the plant leaf weight. The results obtained can be summarized as follows:

1. The characterization of the clay by XRD and the free-swelling tests clearly demonstrates that the clay is expansive.
2. The evolution of the swelling rate of the expansive clay depends strongly on the added fibre content and the loading pressure.
3. Soil samples treated with DISS have significantly lower swelling potential and swelling pressure than the reference sample. Both the swelling potential and swelling pressure decreased when increasing the DISS fibre content.
4. The experimental analysis of the composites shows that the incorporation of plant fibres reduced the weight of the clay samples. The addition of treated fibres in the clay reduced its density and increased its porosity.
5. The increase in the percentage of fibres resulted in a 74% decrease in the angle of friction, but this was offset by an increase in cohesion of 50% compared to the reference sample. In a way, the presence of fibre makes the behaviour similar to that of an undrained soil.
6. The compressive strength was reduced by the addition of DISS fibres, but the ductility of the soil was increased.
7. The incorporation of the fibres increased the optimal water content and reduced the maximum density, resulting in a flattening of the Proctor curves. This result is similar to the treatment of soils by the incorporation of hydraulic binders (choice and/or cement), a very common technique in highway construction projects.
8. The results of this study show that treated natural fibres can be effective reinforcements in the stabilization of expansive soils and can be used in various applications.
9. The results of the study also show that a fibre percentage of 2% is recommended and is effective at reducing the potential for swelling.

References

1. Gaspard K, Mohammad L, Wu Z (2003) Laboratory mechanistic evaluation of soil-cement mixtures with fibrillated polypropylene fibers. 82th Annual Meeting
2. Tang C, Shi B, Gao W, Chen F, Cai Y (2007) Strength and mechanical behaviour of short polypropylene fiber reinforced and cement stabilized clay soil. Geotext Geomembr 25(3):194–202
3. Sirivitmaitrie C, Puppala A, Chikyala V, Saride S, Hoyos L (2008) Combined lime and cement treatment of expansive soils with low to medium soluble sulfate levels. American Society of Civil Engineers. In: Proceedings of the GeoCongress. New Orleans. Louisiana, pp 646–653
4. Phanikumar BR, Sharma RS (2004) Effect of fly ash on engineering properties of expansive soils. J Geotech Geoenviron Eng 130(7):764–767
5. Prabakar J, Dendorkar N, Morchhale K (2004) Influence of fly ash on strength behavior of typical soils. Construct Build Mater 18(4):263–267
6. Rao MR, Rao AS, Babu RD (2008) Efficacy of limestabilized fly ash in expansive soils. Ground Improv 161(1):23–29
7. Rao MR, Rao AS, Babu RD (2008) Efficacy of cement stabilized fly ash cushion in arresting heave of expansive soils. Geotech Geol Eng 26(1):189–197
8. Manikandan R, Ramamurthy K (2009) Swelling characteristic of bentonite on pelletization and properties of fly ash aggregates. J Mater Civ Eng 21(10):578–586
9. Miller G, Azad S (2000) Influence of soil type on stabilization with cement kiln dust. Constr Build Mater 14(2):89–97
10. Ebrahimi A, Edil T, Son Y (2012) Effectiveness of cement kiln dust in stabilizing recycled base materials. Am Soc Civ Eng 24(8):1059–1066
11. Little DN (1996) Assessment of situ structural properties of lime stabilization clay subgrades. Transp Res Rec USA 1546:13–23
12. Mahasneh BZ (2004) Dead Sea water as a soil improvement agent. Electron J Geotech Eng 9:1
13. Arumairaj PD, Sivajothi A (2011) Effect of sea water on expansive soils. Electron J Geotech Eng 15:425–438
14. Otoko GR (2014) The efect of salt water on the physical properties. Compaction characteristics and unconined compressive strength of a clay. Clayey sand and base course. Eur Int J Sci Technol 3(2):9–16
15. Mohamed M, Hussein A (2016) Effect of different water types on expansive soil behavior. Life Sci J 13(5):89–94
16. Horrocks AR, Anand SC (2000) Handbook of technical textiles. Woodhead Publishing Limited in Association with the Textile Institute Abington Hall, Abington
17. Dasaka SM, Sumesh KS (2011) Effect of coir fiber on the stress–strain behavior of a reconstituted fine-grained soil. J Nat Fibers 8(3):189–204
18. Maity J, Chattopadhyay BC, Mukherjee SP (2011) Variation of compaction characteristics of sand randomly mixing with various natural fibers. In: Proceedings of Indian geotechnical conference, December 15–17, Kochi, No. H-287
19. Gray DH, Ohashi H (1983) Mechanics of fiber reinforcement in sand». J Geotech Eng 109(3):335–353
20. Marandi SM, Bagheripour MH, Rahgozar R, Zare H (2008) Strength and ductility of randomly distributed palm fibers reinforced silty-sand soils. Am J Appl Sci 5(3):209–220
21. Ghavami K, Toledo Filho RD, Barbosa NP (1999) Behavior of composite soil reinforced with natural fibres. Cem Concr Compos 21:39–48
22. Santhi Krishna K, Sayida MK (2009) Behavior of black cotton soil reinforced with Sisal fibre. In: 10th National conference on

technological trends (NCTT09), pp 6–7, College of Engineering Trivandrum, India
23. Khelifi Z (2017) Contribution à l'étude du comportement des sols renforcés à l'aide des fibres végétales d'alfa (PhD Thesis). Université Aboubekr Belkaïd, Tlemcen, Algeria
24. Hamrouni A, Dias D, Sbartai B (2018) Reliability analysis of a mechanically stabilized earth wall using the surface response methodology optimized by a genetic algorithm. Geomech Eng 15(4):937–945
25. Hamrouni A, Dias D, Sbartai B (2020) Soil spatial variability impact on the behaviour of a reinforced earth wall. Front Struct Civ Eng (**in press**)
26. Hamrouni A, Dias D, Sbartai B (2019) Probability analysis of shallow circular tunnels in homogeneous soil using the surface response methodology optimized by a genetic algorithm. Tunnell Undergr Space Technol 86:22–33
27. Sivakumar Babu GL, Vasudevan AK, Haldar S (2008) Numerical simulation of fiber-reinforced sand behavior. Geotext Geomembr 26:181–188
28. Gheris A, Meksaouine M (2011) The use of a mixed scheme: mixed hybrid finite elements method/finite volumes (MHFE/FV), for the modeling of contaminants transport in unsaturated porous mediums. Arab J Geosci 4:669–680. https://doi.org/10.1007/s12517-010-0245-8
29. NF P94-041 (1995) Identification granulométrique, tamisage par voie humide. Association françaises de normalisation, AFNOR. ISSN 0335-3931
30. NF P94-057 (1992) Identification granulométrique, méthode par sédimentation. Association françaises de normalisation, AFNOR. ISSN 0335-3931
31. NF P94-051 (1993) Détermination des limites d'Atterberg. Association françaises de normalisation, AFNOR. ISSN 0335-3931
32. NF P94-071-1 (1994) Essai de cisaillement rectiligne à la boite, cisaillement direct. Association françaises de normalisation, AFNOR. ISSN 0335-3931
33. NF P94-090-1 (1997) Essai oedométrique, essai de compressibilité sur matériaux fins quasi saturés avec chargement par paliers. Association françaises de normalisation, AFNOR. ISSN 0335-3931
34. NF P94-093 (1999) Détermination des références de compactage d'un matériau, Essai Proctor normal-Essai Proctor modifié. Association françaises de normalisation, AFNOR. ISSN 0335-3931
35. Sellami A, Merzoud M, Amziane S (2013) Improvement of mechanical properties of green concrete by treatment of the vegetals fibers. Constr Build Mater 47:1117–1124
36. Merzoud M, Habita MF (2007) Elaboration of a lignocellulosic composite formulated with a local ressource: DISS as infill in structures submitted to seismic actions. Res J Appl Sci Medwell J 4:2410–2415
37. Boukhoulda A, Boukhoulda FB, Makich H, Nouari M, Haddag B (2017) Microstructural and mechanical characterizations of natural long alfa fibers obtained with different extractions processes. J Nat Fibers. https://doi.org/10.1080/15440478.2017.1302384
38. Building Research Establishment (1980) Low-rise buildings on shrinkable clay soils: Part 1. BRE Digest 240. HMSO, London
39. Chen FH, Ma GS (1987) Swelling and shrinking behaviours of expansive clays. In: International conference on expansive soils. New Delhi, pp 127–129
40. Seed RJ (1962) Woodward & R.de Lundgren. Prediction of swelling potentiel for compacted clays. J Soil Mech Found Div ASCEJ Soil Mech Found Div ASCE 88:107–131
41. Williams AB, Donaldson GW (1980) Developments related to building on expansive soils in South Africa. In: Proceedings of the 4th international conference on expansive soils. Denver vol 2, pp 834–844
42. NF P94-091 (1995) Essai de gonflement à l'oedométre, determination des déformations par chargement de plusieurs éprouvettes. Association françaises de normalisation, AFNOR. ISSN 0335-3931
43. Gourouza M, Zanguina A, Natatou I, Boos A (2013) Rev. CAMES – Sciences Struct. Mat. 1. Déc. 29
44. Sadki H, Ziat K, Saidi MJ (2014) Mater. Environ Sci 5(S1):2061
45. Boumehraz MA, Mellas M, Goudjil K, Boucetta F (2019) Durability of GCB concrete exposed to sea water sulphates in the region of Jijel, Algeria. Int J Mater 6
46. Zangue Adija H (2012) Univ. Lorraine. Eco. Doc. Scien. Et Ing des Ress. Proc. Prod et Env. 132
47. Arib A, Sarhiri A, Moussa R, Remmal T, Gomina MCR (2007) Chimie 10:504
48. Kohler E (2005) Univ. Evry Val d'Essonne. Eco. Doc. Phys. Chim
49. Sazhin VS (1969) Special construction on subsiding and swelling soils. Osnovaniya, Fundamenty i Mekhanika Gruntov 1969:22–23 **(in Russian)**
50. Lytton RL (1971) Risk design of stiffened mats on clay. In: Proceedings, conference on application of statistics and probability to soil and structural engineering, Hong Kong, pp 153–171
51. Lytton RL, Meyer KT (1971) Stiffened mats on expansive clay. ASCE J Soil Mech Found Div 97(n° SM7):999–1017
52. Ali A, Benelmir R, Tanguier J-L, Todjiba AS (2017) Caractéristiques mécaniques de l'argile de Ndjamena stabilisée par la gomme arabique. Afrique Sci J 13(5):330–341